MOEM

Modern Electronic Materials 2021; 7(3): 85–89
DOI 10.3897/j.moem.7.3.75786

Research Article

Magnetization of magnetically inhomogeneous $Sr_2FeMoO_{6-\delta}$ nanoparticles

Gunnar Suchaneck[1]

1 TU Dresden, Solid State Electronics Laboratory, 01062 Dresden, Germany

Corresponding author: Gunnar Suchaneck (Gunnar.Suchaneck@tu-dresden.de)

Received 3 September 2021 ♦ **Accepted** 26 September 2021 ♦ **Published** 30 September 2021

Citation: Suchaneck G (2021) Magnetization of magnetically inhomogeneous $Sr_2FeMoO_{6-\delta}$ nanoparticles. Modern Electronic Materials 7(3): 85–89. https://doi.org/10.3897/j.moem.7.3.75786

Abstract

Magnetization is a key property of magnetic materials. Nevertheless, a satisfactory, analytical description of the temperature dependence of magnetization in double perovskites such as strontium ferromolybdate is still missing. In this work, we develop, for the very first time, a model of the magnetization of nanosized, magnetically inhomogeneous $Sr_2FeMoO_{6-\delta}$ nanoparticles. The temperature dependence of magnetization was approximated by an equation consisting of a Bloch-law spin wave term, a higher order spin wave correction, both taking into account the temperature dependence of the spin-wave stiffness, and a superparamagnetic term including the Langevin function. In the limit of pure ferromagnetic behavior, the model is applicable also to SFMO ceramics. In the vicinity of the Curie temperature ($T/T_C > 0.85$), the model fails.

Keywords

nanoparticles, magnetization, strontium ferromolybdate.

1. Introduction

Strontium ferromolybdate ($Sr_2FeMoO_{6-\delta}$ – **SFMO**) is the most studied ferrimagnetic double perovskite. SFMO double perovskites are promising candidates for magnetic electrode materials for room-temperature spintronics applications, because they present a half-metallic character (with theoretically 100% polarization), a high Curie temperature (T_C) of about 415 K (ferromagnets should be operated in their ordered magnetic state below T_C), and a low-field magnetoresistance [1]. However, a wide application of SFMO is still missing because of the low reproducibility of its magnetic properties originating in ceramic processing issues and its aging in contact with air and moisture.

Magnetic nanoparticles are building units of spintronic devices, magnetic sensors, radio-frequency and microwave devices, biomedical sensing and photonic systems, etc. Depending on particle, element or island size, magnetic properties change sufficiently. Below a certain size, the element first takes a single-domain state while in an ensemble of nanoparticles a superparamagnetic state appears at smaller sizes in dependence on temperature and observation (measurement) time. In the latter state, demagnetization occurs without coercivity since it is caused by thermal energy and not by the application of a magnetic field. Thus, the memory of the remanent state of the element is lost [2].

Magnetization characterizes the density of permanent or induced magnetic dipole moments in a magnetic material. In granular magnetic films, magnetization determines the magnetoresistance [3] which is the key property for SFMO application in magnetic memories and magnetic sensors.

© 2021 National University of Science and Technology MISiS. This is an open access article distributed under the terms of the Creative Commons Attribution License (CC-BY 4.0), which permits unrestricted use, distribution, and reproduction in any medium, provided the original author and source are credited.

Up to now, there is no satisfactory analytical expression for the relative magnetization $m(T)$, i.e. the magnetization M scaled to the saturation magnetization M_s, except for the two limiting cases, $t \to 0$ and $t \to 1$, where $t = T/T_C$ with T_C the Curie temperature is the reduced temperature. In the first case, a function

$$m(T) = \left[1 - st^{3/2} - (1-s)t^p\right]^{1/3}, \tag{1}$$

proposed for ferromagnetic metals and alloys [4] is suitable, where the term

$$m(T) = \left(1 - st^{3/2}\right)^{1/3} \tag{2}$$

corresponds to Bloch´s 3/2 power law for non-interacting spin waves (magnons) at low temperatures [5]. Here, s and p in Eq. (1) are fit parameters, $s > 0$ and $p > 3/2$. The adjustable parameter p was found to be $p = 5/2$ for Co, Ni, Gd, YCo_5, Y_2Fe_{17}, GdZn, while for Fe $p = 4$. The slope factor s can be estimated also by means of semi-classical linear spin wave theory yielding [4, 6–8]

$$s = \frac{1}{4}\pi^{-3/2} Z_{3/2}(x) \frac{\mu_B}{M_0}\left(\frac{kT_C}{D}\right)^{3/2}, \tag{3}$$

with μ_B the Bohr magneton, M_s the saturation magnetization, k the Boltzmann constant, and D the effective spin wave stiffness coefficient, and the function

$$Z_p(x) = \sum_{n=1}^{\infty} n^{-p} \exp(-nx), \tag{4}$$

representing the polylogarithm function $\mathrm{Li}_p(\xi)$ with an argument of $\xi = \exp(-x)$. In the low field limit ($x \to 1$), $Z_{3/2}(x)$ with $x = \mu_B B/kT$ reduces to the Riemann zeta function $\zeta(3/2)$. For SFMO, D at low temperatures (0.4 to 10 K) amounts to about $1.4 \cdot 10^{-21}$ eVm^2 [9]. Quoting M_s in terms of the number of Bohr magnetrons per formula unit and taking $M_s \approx 4\ \mu_B$/f.u. and $T_C = 415$ K [1], we obtain $s = 0.477$ for $B \to 0$. On the other hand, fitting Eq. (2) to experimental data of SFMO [1, 10, 11] yields $s = 0.675$.

For SFMO, Eqs. (1) and (2) coincides up to about 120 K while reproducing the experimental $m(T)$ behavior [1, 10, 11] very well up to about 50 K (Fig. 1). At higher temperature, the slope $\mathrm{d}m(T)/\mathrm{d}T$ becomes smaller than the experimental one, while the slope of Eq. (1) near T_C exceeds the experimental value significantly. The last term in Eq. (1) represents for $p = 5/2$ a higher order correction to the Bloch formula arising from the discreteness of the lattice [6]. This last term may be replaced also by a T^2 term attributed to collective electron behavior [12]. Here, a distinction between T^2 and $T^{5/2}$ terms can hardly be made since both terms equally well describe the experimental data.

The simulation of the temperature dependent magnetization by Monte Carlo methods and Landau–Lifshitz–Gilbert atomistic spin models [13] yields

$$m(T) = \left(1 - t\right)^{1/3}. \tag{5}$$

This relationship provides for SFMO an initial starting point for $m(T)$ calculation (cf. Fig. 1). In this case, the inclusion of higher order terms makes the approximation worse.

For $T \to T_C$, the low field limit of $m(T)$ is given by [14]

$$m(T) = c\left(1 - t\right)^{\beta}, \tag{6}$$

where $\beta_{SFMO} = 1/2$ [10]. This results in $c \approx \sqrt{3}$.

An empirical interpolation formula of $m(T)$ for iron whiskers was presented [15]:

$$m(T) = \frac{\left(1-t\right)^{\beta}}{1 - \beta T + At^{3/2} - Ct^{7/2}}, \tag{7}$$

which matches the experimental behavior $m(T) = (1 - At^{3/2})$ at $t \to 0$ with $m(T) \propto (1 - t)^{\beta}$ at $t \to 1$.

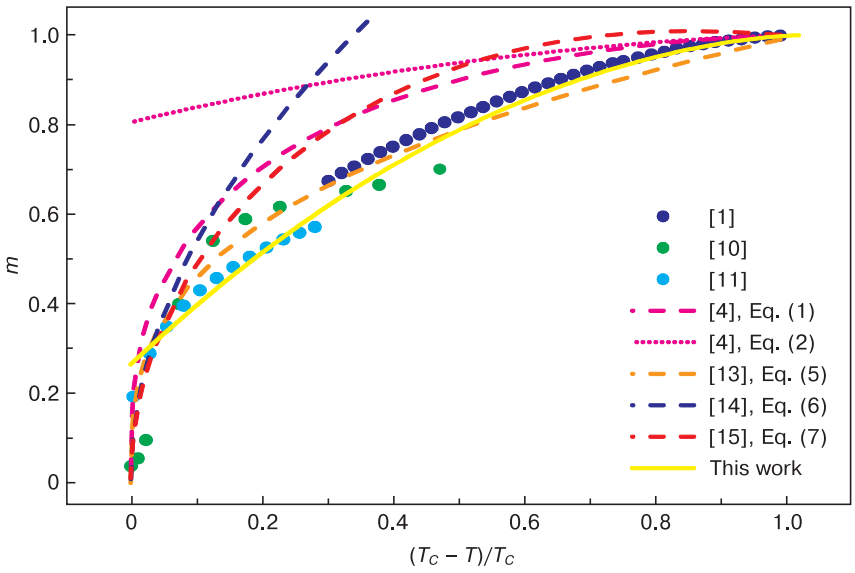

Figure 1. Temperature dependence of the reduced magnetization of SFMO according to Eq. (1), (2), (5), (6), and (7) in comparison with experimental data [1, 10, 11].

The $t^{7/2}$ term was chosen to improve the fit to the experimental data. Thereby, the coefficient C was determined by matching the interpolation formula and the $t \to 0$ behavior for $t \to 1$. Both, Eq. (6) and Eq. (7) are not suitable approximations for SFMO.

Figures 1 compares values of $m(T)$ calculated by means of the discussed above equations with experimental data [1, 10, 11] and the model of this work for pure ferrimagnetic behavior. In order to compare samples with different T_C, a reduced temperature scale $(T_C–T)/T_C$ was applied. Only Eq. (5) and the model of this work provide satisfactory results.

Recently, an inhomogeneous magnetic state was obtained in SFMO nanoparticles fabricated by solid-state reaction from partially reduced $SrFeO_{3-x}$ and $SrMoO_4$ precursors studying the temperature dependences of the magnetization measured in the field-cooling **(FC)** and zero-field-cooling **(ZFC)** modes and small-angle neutron scattering [16]. This state was attributed to the frustration of the exchange bonds and the realization of various magnetic states – antiferromagnetic, ferrimagnetic, and superparamagnetic, when the spin inversion does not change the energy of the system in a wide range of temperatures. In another report by [17], the Mössbauer spectrum of SFMO fine particles of about 30 nm size consisting of small traces of $SrMoO_4$ revealed a paramagnetic doublet above a blocking temperature of 45 K, while the spectrum of a similar sample with a size of 197 nm taken at 77 K included superparamagnetic, ferrimagnetic and surface contributions. The coexistence of different magnetic phases – superparamagnetic, ferromagnetic and paramagnetic – was revealed in single phase $Mg_xZn_{1-x}Fe_2O_4$ nanoparticles by Mössbauer spectroscopy and curve fitting of the magnetic field dependence of the magnetization [18]. It was attributed to the distribution of particle size in the samples. Other magnetically inhomogeneous systems with ferroelectric and superparamagnetic components include, for instance, composites of Co–P alloy with ultradispersed corundum and detonation nanodiamond [19].

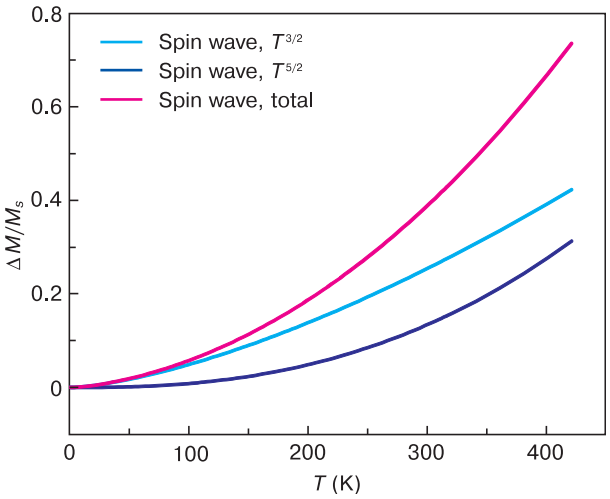

Figure 2. Fractional change of magnetization $\Delta M/M_s$ induced by the spin-wave $T^{3/2}$ and $T^{5/2}$ terms of Eq. (8).

In this work, a model is developed which describes the temperature dependence of magnetization of nanosized and magnetically inhomogeneous SFMO nanoparticles.

2. Methods

The temperature dependence of the reduced magnetization M/M_s when measured in the FC mode was approximated by an equation consisting of a Bloch-law spin-wave term, a higher order spin-wave correction, and a superparamagnetic term including the Langevin function L [19]

$$m(T) = m_{FM}\left(1 - ET^{3/2} - FT^{5/2}\right) + \\ + m_{SPM}L\left(\frac{\mu_{\text{eff}}B}{kT}\right), \quad (8)$$

where m_{FM} is the reduced ferrimagnetic magnetization, $m_{SPM} = N_{SPM}\mu_{\text{eff}}/M_s$ the reduced superparamagnetic magnetization of N_{SPM} particles, and μ_{eff} the effective magnetic moment of the superparamagnetic phase which is a fitting parameter in the order of $3 \cdot 10^4$ μ_B [20]. Contrarily to [19], we do not fit the coefficients E and F to experimental data, but calculate them by means of spin-wave theory. In the long wavelength approximation, the coefficients E and F are given [6, 12, 21]

$$E = \frac{g\mu_B V}{M_s} Z_{3/2}\left(\frac{\mu_B B}{kT}\right)\left(\frac{k}{4\pi D}\right)^{3/2}, \quad (9)$$

where g is the Landé spitting factor, and V the volume of a unit cell given by

$$V = \frac{M_{SFMO}}{\rho_{SFMO}N_A}, \quad (10)$$

with M the molar mass, ρ the density and N_A the Avogadro constant, and

$$F = \frac{3\pi}{4}\frac{g\mu_B V}{M_s}\left\langle r^2\right\rangle Z_{5/2}\left(\frac{\mu_B B}{kT}\right)\left(\frac{k}{4\pi D}\right)^{5/2}, \quad (11)$$

where $\langle r^2\rangle$ is a the range of exchange interaction amounting for only nearest-neighbor exchange $\langle r^2\rangle = a^2 = V^{2/3}$ with a the lattice parameter of one unit cell. Here, the saturation magnetization M_s is quoted in terms of the number of Bohr magnetrons per formula unit. The temperature dependence of the spin-wave stiffness constant is given by [21, 22]:

$$D(T) = D(0)\left[1 - \pi\left\langle r^2\right\rangle\frac{g\mu_B}{M_s}Z_{5/2} \times \right. \\ \left. \times \left(\frac{\mu_B B}{kT}\right)\left(\frac{kT}{4\pi D(0)}\right)^{5/2}\right]. \quad (12)$$

Also here, the long wavelength approximation was considered. The decrease of $D(T)$ with temperature increases the coefficients E and F. In manganites close in the vicinity of T_C, Eq. (12) overestimates $D(T)$ significantly [23] limiting the temperature range of the model

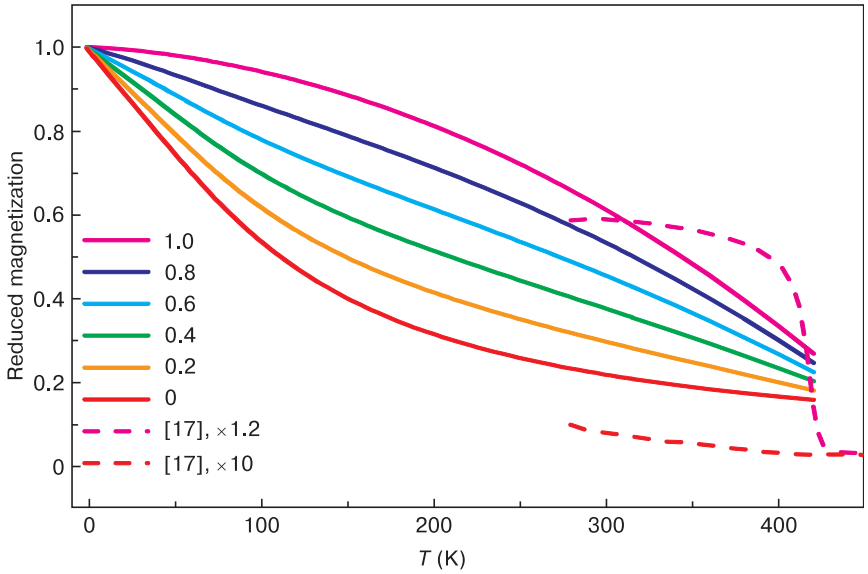

Figure 3. $m(T)$ calculated by means of Eq. (8) for different fractions ξ.

to $t \leq 0.85$. Note that the coefficients of the $T^{5/2}$ term in Eqs. (11) and (12) are identical except for the numerical factor of 3/4.

3. Results and discussion

For all calculations, the Curie temperature was fixed to T_C = 420 K, the saturated magnetization to M_s = 3.75 μB/f.u., the the Landé spitting factor g to $g \approx 2$, the low temperature spin-wave stiffness constant to $D(0) = 1.4 \cdot 10^{-21}$ eVm^2, the range of exchange interaction to $\langle r^2 \rangle = a^2$, the magnetic flux density to B = 10 mT, and the effective magnetic moment of the superparamagnetic phase to $\mu_{eff} = 3 \cdot 10^4\ \mu_B$. The latter corresponds $1.18 \cdot 10^4$ spins in a particle of a volume of about 1460 nm^3. Figure 2 illustrates the fractional change of magnetization $\Delta M/M_s$ of ferromagnetic SFMO induced by the spin-wave $T^{3/2}$ and $T^{5/2}$ terms of Eq. (8). Above 200 K, the values of $\Delta M/M_s$ are probably slightly overestimated since the appearance of magnetic disorder in SFMO induces a pronounced extrinsic damping of spin waves [24]. On the other hand, above 360 K in the vicinity of the Curie temperature, $\Delta M/M_s$ will be significantly larger than predicted as a result of an incorrect description of $D(T)$, Eq. (12), in this temperature range.

Figure 3 compares values of $m(T)$ calculated by means of Eq. (8) for different fractions $\xi = FM(FM + SPM)$. For sake of simplicity, we have assumed $M_s^{SPM} = M_s^{FM}(1 - \xi)$. The $m(T)$ behavior changes from a curve with increasing with temperature slope to a curve with decreasing with temperature slope. This change in the curve shape is in qualitative agreement with the one obtained in [17]. A quantitative comparison is not possible since the difference in the values of M_s^{FM} and M_s^{SPM} is not known. For $\xi = 1$ the model describes ferrimagnetic SFMO without any fitting parameter (cf. Fig. 1). Here, the agreement with experiment can be improved by using more reliable physical parameters, taking into account the damping of spin waves by magnetic disorder and improving modeling of the spin-wave stiffness constant $D(T)$ in the vicinity of the Curie temperature.

4. Conclusions

Magnetically inhomogeneous nanoparticles can be analyzed by measuring the temperature dependence of the magnetization. A model for the determination of ferrimagnetic and superparamagnetic fractions of SFMO nanoparticles is presented in this work. In the limit of pure ferrimagnetic behavior, the model is applicable also to SFMO ceramics. However, it overestimates the magnetization change at higher temperatures (> 200 K) since the appearance of magnetic disorder in SFMO induces a pronounced extrinsic damping of spin waves [24]. In the vicinity of the Curie temperature ($T/T_C > 0.85$), the model fails. The model provides a base for the design of spintronic devices, magnetic sensors as well as for medical application of magnetic particles, e.g., contrast agents in clinical MRI magnetic resonance imaging or local heating using strong magnetic AC-fields (hyperthermia).

Acknowledgements

This research was funded by the European Union within the scope of the European project H2020-MSCA-RISE-2017-778308–SPINMULTIFILM. The author has benefited from valuable discussions with N.A. Sobolev, N.A. Kalanda and E. Artiukh.

References

1. Kobayashi K.-I., Kimura T., Sawada H., Terakura K., Tokura Y. Room-temperature magnetoresistance in an oxide material with an ordered double-perovskite structure. *Nature*, 1998; 395: 677–680. https://doi.org/10.1038/27167
2. O'Handley R.C. Modern Magnetic Materials: Principles and Applications. New York: Wiley, 2000, 740 pp.
3. Inoue J., Maekawa S. Theory of tunneling magnetoresistance in granular magnetic films. *Phys. Rev. B*, 1996; 53(18): R11927–R11929. https://doi.org/10.1103/PhysRevB.53.R11927
4. Kuz'min M.D. Shape of temperature dependence of spontaneous magnetization of ferromagnets: Quantitative analysis. *Phys. Rev. Lett.*, 2005; 94(10): 107204. https://doi.org/10.1103/PhysRevLett.94.107204
5. Bloch F. Zur Theorie des ferromagnetismus. *Zeitschrift für Physik*, 1930; 61: 206–219. https://doi.org/10.1007/BF01339661
6. Dyson F.J. Thermodynamic behavior of an ideal ferromagnet. *Phys. Rev.*, 1956; 102(5): 1230–1244. https://doi.org/10.1103/PhysRev.102.1230
7. Williams G., Loram J.W. Estimates of the acoustic spin wave stiffness from electrical resistivity measurements on dilute PdFe, PdCo and PdMn alloys. *J. Physics F: Metal Physics*, 1971; 1(4): 434–443. https://doi.org/10.1088/0305-4608/1/4/316
8. Kittel C. Introduction to Solid State Physics. New York: Wiley, 2005: 334.
9. Tomioka Y., Okuda T., Okimoto Y., Kumai R., Kobayashi K.-I., Tokura Y. Magnetic and electronic properties of a single crystal of ordered double perovskite Sr_2FeMoO_6. *Phys. Rev. B*, 2000; 61(1): 422–427. https://doi.org/10.1103/PhysRevB.61.422
10. Navarro J., Nogués J., Muñoz J.S., Fontcuberta J. Antisites and electron-doping effects on the magnetic transition of Sr_2FeMoO_6. *Phys. Rev. B*, 2003; 67(17): 174416. https://doi.org/10.1103/PhysRevB.67.174416
11. Serrate D., De Teresa J.M., Algarabel P.A., Ibarra M.R., Galibert J. Intergrain magnetoresistance up to 50 T in the half-metallic $(Ba_{0.8}Sr_{0.2})_2FeMoO_6$ double perovskite: Spin-glass behavior of the grain boundary. *Phys. Rev. B*, 2005; 71(10): 104409. https://doi.org/10.1103/PhysRevB.71.104409
12. Argyle B.E., Charap S.H., Pugh E.W. Deviations from $T^{3/2}$ law for magnetization of ferrometals: Ni, Fe, and Fe+3% Si. *Phys. Rev.*, 1963; 132(5): 2051–2062. https://doi.org/10.1103/PhysRev.132.2051
13. Evans R.F.L., Fan W.J., Chureemart P., Ostler T.A., Ellis M.O.A., Chantrell R.W. Atomistic spin model simulations of magnetic nanomaterials. *J. Phys.: Condens. Matter*, 2014; 26(10): 103202. https://doi.org/10.1088/0953-8984/26/10/103202
14. Arrott A., Noakes J.E. Approximate equation of state for nickel near its critical temperature. *Phys. Rev. Lett.*, 1967; 19(14): 786–789. https://doi.org/10.1103/PhysRevLett.19.786
15. Arrott A.S., Heinrich B. Application of magnetization measurements in iron to high temperature thermometry. *J. Appl. Phys.*, 1981; 52(3): 2113–2115. https://doi.org/10.1063/1.329634
16. Kalanda N., Karpinsky D., Bobrikov I., Yarmolich M., Kuts V., Huang L., Hwang C., Kim D.-H. Interrelation among superstructural ordering, oxygen nonstoichiometry and lattice strain of double perovskite $Sr_2FeMoO_{6-\delta}$ materials. *J. Mater. Sci.*, 2021; 56: 11698–11710. https://doi.org/10.1007/s10853-021-06072-0
17. Suominen T., Raittila J., Salminen T., Schlesier K., Lindén J., Paturi P. Magnetic properties of fine SFMO particles: Superparamagnetism. *J. Magn. Magn. Mater.*, 2007; 309(2): 278–284. https://doi.org/10.1016/j.jmmm.2006.07.016
18. John S.P., Mathew J. Determination of ferromagnetic, superparamagnetic and paramagnetic components of magnetization and the effect of magnesium substitution on structural, magnetic and hyperfine properties of zinc ferrite nanoparticles. *J. Magn. Magn. Mater.*, 2019; 475: 160–170. https://doi.org/10.1016/j.jmmm.2018.11.030
19. Goncharova O.A., Chekanova L.A., Denisova E.A., Komogortsev S.V., Iskhakov R.S., Eremin E.V. Ferromagnetic Co-P powders with nanodiamond and corundum precipitates. *Solid State Phenomena*, 2012; 190: 470–473. https://doi.org/10.4028/www.scientific.net/SSP.190.470
20. Caizer C. Magnetic behaviour of $Mn_{0.6}Fe_{0.4}Fe_2O_4$ nanoparticles in ferrofluid at low temperatures. *J. Magn. Magn. Mater.*, 2002; 251: 304–315. https://doi.org/10.1016/S0304-8853(02)00701-1
21. Marshall W. Spin Ordering. In: Davies R.O. (Ed.) *Proceedings of the 8th International Confonference on Low Temperature Physics*. London: Butterworth Inc., 1963: 215–219.
22. Weber R., Tannenwald P.E. Long-range exchange interactions from spin-wave resonance *Phys. Rev.*, 1965; 140(2A): A498–A506. https://doi.org/10.1103/PhysRev.140.A498
23. Vasiliu-Doloc L., Lynn J.W., Mukovskii Y.M., Arsenov A.A., Shulyatev D.A. Spin dynamics of strongly doped $La_{1-x}Sr_xMnO_3$. *J. Appl. Phys.*, 1998; 83(11): 7342—7344. https://doi.org/10.1063/1.367634
24. Nosach T., Mullady G., Leifer N., Adyam V., Li Qi, Greenbaum S., Ren Y. Angular dependence of spin-wave resonance and relaxation in half-metallic Sr_2FeMoO_6 films. *J. Appl. Phys.*, 2008; 103(7): 07E311. https://doi.org/10.1063/1.2837030